

Electronic excitations in alkali-metal overlayers. I. Unreconstructed low-temperature phase of Li/Al

H. Ishida

College of Humanities and Sciences, Nihon University, Sakura-josui, Tokyo 156, Japan

A. Liebsch

Institut für Festkörperforschung, Forschungszentrum, 52425 Jülich, Germany

(Received 4 November 1997)

The influence of interband transitions on collective excitations in adsorbed alkali-metal layers is investigated for Li on Al in the unreconstructed low-temperature phase. The three-dimensional Li overlayer is described in terms of nonlocal pseudopotentials while the Al substrate is treated within the jellium model. The finite-frequency response appropriate for incident photons is calculated within the time-dependent density-functional approach. In striking contrast to previous results for Na and K layers on Al, which reveal multipole surface and bulklike overlayer plasmons, we find for Li overlayers only one dominant adsorbate-induced collective excitation associated with the Li multipole surface plasmon. The bulklike Li overlayer plasmon is greatly suppressed due to single-particle transitions induced by the Li lattice potential. The theoretical spectra compare well with recent photoyield measurements for Li on Al(111). [S0163-1829(98)10519-2]

I. INTRODUCTION

Electronic excitations in thin alkali-metal overlayers can be studied using a variety of techniques. A frequently employed method is electron energy-loss spectroscopy (EELS),¹ which, in principle, allows one to map out the q_{\parallel} dispersion of the adsorbate-induced modes for a wide range of coverages (q_{\parallel} denotes the two-dimensional wave number). However, as will be discussed in the subsequent section, the interpretation of loss spectra at $q_{\parallel} \approx 0$ is nontrivial. On the other hand, photoyield or photoemission measurements are suited for studying the excitation spectra in the long-wavelength limit ($q_{\parallel} = 0$). In the past, such studies have been used mainly to investigate the nature of the occupied alkali-metal states, in particular, the quantum-well states formed on noble metal substrates.² Adsorbate-induced excitations have also been detected as satellites in core-level photoemission spectra.³ Although these spectra reveal interesting shifts of loss features due to temperature-induced structural rearrangements, this technique provides no information on the q_{\parallel} dispersion of overlayer collective modes. Thus, in spite of nearly three decades of research,⁴ the understanding of adsorbate-induced excitations is much less developed than those on clean semi-infinite metals.⁵

Very recently, this situation greatly improved when surface photoyield measurements for K on Al by Kim, Plummer, and Liebsch⁶ and for Na and K on Al by Barman *et al.*⁷ were carried out over a wide range of photon energies. These data fully confirmed theoretical predictions by Liebsch⁸ and Ishida and Liebsch⁹ based on the time-dependent local-density approximation (TDLDA).¹⁰ Roughly three coverage regions exhibiting distinct excitation spectra can be identified. In the submonolayer regime, the calculated spectra reveal only a broad feature associated with the so-called *threshold excitation*, i.e., when the photon energy approaches the work function Φ of the system. In this coverage range

the spectral frequency and the average electron density of the adsorbate are not simply related via $\omega \sim \sqrt{4\pi n}$. It is not meaningful to speak of a well-defined overlayer surface plasmon. Near about one monolayer, the spectral feature rapidly shifts to higher frequencies. Finally, for about two or more monolayers, two collective modes appear: the bulklike overlayer plasmon near the alkali-metal volume plasma frequency ω_p , and the multipole surface plasmon near $\omega_m \approx 0.8 \omega_p$. The results of both experimental groups^{6,7} are in excellent agreement with these predictions. In addition, the data show that for increasing overlayer thickness, the intensity of the bulklike mode diminishes. This observation is consistent with previous experimental and theoretical results for yield spectra of semi-infinite alkali metals¹¹⁻¹³ according to which the photoemitted yield for $\omega = \omega_p$ is at a minimum. The local-field enhancement associated with the multipole surface mode at ω_m then becomes the dominant electronic surface excitation.

The physical reason for the appearance of two collective modes near ω_p and ω_m at a coverage of about two or more monolayers is that the density in the overlayer is rather flat and the adsorbate interfaces are well separated. A bulklike plasma oscillation within the overlayer is then feasible. This mode is analogous to the antisymmetric collective mode of a finite slab. Moreover, the density profile at the adsorbate-vacuum interface is nearly the same as on the semi-infinite alkali-metal surface, so that the multipole surface plasmon becomes a well-defined excitation. In the case of Na and K overlayers, lattice effects on the yield spectra are very weak.⁹ Thus, the overlayer excitations can be well understood in terms of the jellium model for alkali-metal adsorption.¹⁴

In sharp contrast to Na and K, Li overlayers on Al(111) reveal excitation spectra that differ qualitatively from the predictions of the jellium model.⁷ Although in the submonolayer regime there is again evidence of the threshold excitation, beyond two monolayers only one clear overlayer col-

lective mode is observed near 5.2 eV. A second spectral feature appears as a weak shoulder on the high-frequency side in the 6–8 eV range. Apart from the surprising relative weights, the frequencies of these features differ greatly from the spectral peaks obtained in the equivalent jellium model. Since the ionic pseudopotential of Li is much stronger than that of Na and K, the spectral modifications suggest a significant coupling of the overlayer collective modes to lattice-induced single-particle transitions.

In this paper we present a detailed analysis of band-structure effects on the electronic excitations of Li overlayers adsorbed on Al. The calculational method is fully three dimensional, and the Li ion cores are described using a norm-conserving pseudopotential.¹⁵ Coverages of two and three Li monolayers are considered, where the Li atoms may be adsorbed either in the (110) or (001) geometry. The electronic excitations are evaluated in the long-wavelength limit appropriate for incident photons, using the TDLDA.¹⁰

The theoretical results indicate that the main Li adsorbate excitation near 5.2 eV corresponds to the multipole surface plasmon, while the high-frequency shoulder is associated with the bulklike overlayer plasmon. Thus, lattice effects on the multipole mode are much weaker than on the Li bulk plasmon. This finding is rather unexpected since available photoyield and electron energy-loss spectra on clean metal surfaces suggest that the multipole surface plasmon is a fragile surface excitation readily weakened by interband transitions. For instance, nearly-free-electron metals such as Na, K, Cs, Al, and Mg show the multipole mode.^{5,11,12,16,17} On the other hand, metals exhibiting substantial lattice effects such as Li,¹⁷ Ag,¹⁸ and Hg (Ref. 19) do not reveal any clear evidence of it. Thus, large pseudopotentials, occupied d bands, or shallow core levels appear to annihilate this surface excitation. The present results demonstrate instead that the Li multipole mode exists in spite of strong lattice effects. Surprisingly, the overlayer bulklike plasmon is nearly suppressed due to interference with interband transitions. The origin of this behavior is connected with the location of the fluctuating charge densities. Since the multipole mode is confined to the overlayer-vacuum interface, it is largely decoupled from interband transitions. In contrast, the bulklike mode corresponds to a standing wave that extends across the entire overlayer. It is therefore fully exposed to the lattice potential. Our results show that, even at a coverage of only two monolayers, this mode has nearly the same frequency and width as the volume plasmon of bulk Li.²⁰ The TDLDA spectra for three-dimensional Li overlayers are in qualitative agreement with the measured yield data. A one-dimensional adsorbate potential that neglects the lattice structure parallel to the surface is shown to underestimate the effect of single-particle transitions on the Li overlayer excitations.

The outline of this paper is as follows. In Sec. II, we first discuss the relationship between theoretical response functions and measured photoyield spectra. Then, we describe the chemisorption model for Li/Al and the computational procedure for calculating the dynamical response properties within the TDLDA. Section III discusses the theoretical results and the comparison with the experimental spectra. A summary is given in Sec. IV. Atomic units are used throughout unless noted otherwise. A preliminary account of the present work is given in Ref. 7.

II. THEORY

A. Surface response functions

We analyze the excitation spectra of adsorbed Li layers on Al in the long-wavelength limit. For convenience, the Al substrate is treated as jellium, since, in the range of Li excitations, the substrate spectrum is very weak and featureless. According to Feibelman,¹³ the power absorption when P -polarized light is shed on the surface is

$$P(\omega) = \frac{\omega}{8\pi} [\epsilon(\omega) - 1] \left[|E_x|^2 \text{Im } d_{\parallel}(\omega) + \frac{1}{\epsilon(\omega)} |D_z|^2 \text{Im } d_{\perp}(\omega) \right], \quad (1)$$

where $\epsilon(\omega) = 1 - \Omega_p^2/\omega^2$ is the dielectric constant of the substrate (Ω_p is the plasma frequency of Al), and E_x (D_z) denotes the x (z) component of the electric field (displacement vector). We choose the z axis as the surface normal pointing toward the vacuum, and the electric field lies in the xz plane. $d_{\perp}(\omega)$ in Eq. (1) is defined as the centroid of $n_1(\mathbf{r}, \omega)$, the charge density induced by a uniform electric field perpendicular to the surface:

$$d_{\perp}(\omega) = \frac{1}{S\sigma(\omega)} \int d\mathbf{r} z n_1(\mathbf{r}, \omega), \quad (2)$$

where $\sigma(\omega) = [\epsilon(\omega) - 1]/[\epsilon(\omega) + 1]$ is the integrated induced charge per unit area and S stands for the surface area. $\text{Im } d_{\perp}(\omega)$ can also be expressed using the golden-rule formula as²¹

$$\text{Im } d_{\perp}(\omega) = \frac{1}{2\sigma(\omega)[\sigma(\omega) + 1]} \times \sum_{i,j} \delta(\epsilon_j - \epsilon_i - \hbar\omega) |\langle \psi_j | \phi_1(\mathbf{r}, \omega) | \psi_i \rangle|^2, \quad (3)$$

where ψ_i and ψ_j denote one-electron wave functions of the occupied and unoccupied states, respectively, and the initial-state energy ϵ_i should be in the interval $[\epsilon_F - \hbar\omega, \epsilon_F]$ (ϵ_F is the Fermi energy). This equation indicates that $\text{Im } d_{\perp}(\omega)$ is proportional to the transition rate for creating electron-hole pair excitations with energy $\hbar\omega$ when a uniform electric field perpendicular to the surface is applied. The collective modes manifest themselves as an enhancement of the self-consistent field $\phi_1(\mathbf{r}, \omega)$. Electrons excited above the vacuum level are partly emitted in the vacuum and detected in photoyield measurements. There also exists the internal channel where excited electrons propagate toward the interior of the metal until they are deexcited. The summation over the final state ψ_j in Eq. (3) includes both the internal and external excitation channels. Fortunately, these channels differ mainly in their intensities but not in the peak positions.^{22,23} Thus, although $\text{Im } d_{\perp}(\omega)$ cannot be used for quantitative analyses of the measured photoyield spectra, it may suffice for qualitatively understanding the observed features.

Electron-hole pair excitations are also created by the parallel components of the electric field and the electrons thus excited contribute to photoyield intensities. $d_{\parallel}(\omega)$ in Eq. (1)

is defined as the centroid of the z derivative of the current density induced by a uniform electric field parallel to the surface. At small ω , $\text{Im } d_{\parallel}(\omega)$ diverges as $1/\omega$ and the coefficient of this divergence is related to the surface resistivity, i.e., the energy dissipation via single-particle excitations when the current flows parallel to the surface.⁹ For a flat jellium surface, $\text{Im } d_{\parallel}(\omega)$ vanishes identically. $\text{Im } d_{\parallel}(\omega)$ becomes finite when conduction electrons incident on the surface from the interior of the metal are scattered off specularly due to potential corrugations in the surface plane.²⁴ For Na and K layers with weak pseudopotentials, $\text{Im } d_{\parallel}(\omega)$ was found to be negligible.⁹ For Li, $\text{Im } d_{\parallel}(\omega)$ is expected to be larger because of the stronger lattice effects.

In the present work we focus on the surface excitations accessible to incident photons, i.e., those with vanishing parallel momentum transfer ($q_{\parallel}=0$). In this limit, EELS spectra are determined by the classical loss function $\text{Im } \sigma(\omega)$, which vanishes except at the monopole surface plasmon frequency of Al, $\Omega_s = \Omega_p / \sqrt{2}$. $\text{Im } d_{\perp}(\omega)$ and $\text{Im } d_{\parallel}(\omega)$ containing the information on the overlayer modes appear as a correction of the order of q_{\parallel} to the classical EELS loss function.¹³ As discussed in Refs. 6 and 8, the principal overlayer mode with frequency $\omega_m \approx 0.8\omega_p$ at $q_{\parallel}=0$ disperses downward with increasing q_{\parallel} and approaches the monopole surface plasmon dispersion of the semi-infinite alkali metal, $\omega_s(q_{\parallel})$, at around $q_{\parallel} = 1/(ca)$ (c is the number of Li layers and a is the lattice spacing between neighboring Li layers). Because of the finite detector aperture, and the vanishing spectral weight of this mode at $q_{\parallel}=0$, the observed EELS peak then consists of a superposition of both multipole and monopole contributions. Thus, the relation between photoyield and loss spectra is highly nontrivial. In particular, as a result of the nonanalytic, negative dispersion of the overlayer modes near $q_{\parallel}=0$, the spectral peaks observed in EELS are redshifted by several tenths of an eV compared to the modes seen in yield spectra. It is therefore, in principle, impossible using EELS to detect the true frequencies of overlayer modes in the $q_{\parallel}=0$ limit.

B. Computational method

As stated above, the Al substrate is treated as semi-infinite jellium in our chemisorption model. On the other hand, the adsorbed Li layers are described fully three dimensionally using a norm-conserving pseudopotential in the Kleinman-Bylander form.¹⁵ The ground-state electronic structure of the system is determined within the embedding scheme of Inglesfield.²⁵ Thus, the asymptotic regions of the semi-infinite substrate and vacuum are handled via complex scattering potentials. To examine the sensitivity of the Li excitations to the structure of the underlying lattice, we consider the (110) as well as (001) adsorption geometries. The distance between Li planes is assumed to be the same as in the bulk ($a_{110} = 2.47 \text{ \AA}$, $a_{001} = 1.75 \text{ \AA}$). The position d of the first Li plane above the substrate jellium edge is determined by minimizing the total energy. We find $d_{110} = 1.64 \text{ \AA}$ and $d_{001} = 1.48 \text{ \AA}$. The electronic excitations are evaluated in the long-wavelength limit ($q_{\parallel}=0$) appropriate for incident photons, using the TDLDA.¹⁰ We determine the linear response of the system to a uniform ac electric field oriented normal as well as parallel to the surface. The computational method is described in detail in Ref. 9 as for $d_{\perp}(\omega)$ and in Ref. 26 as

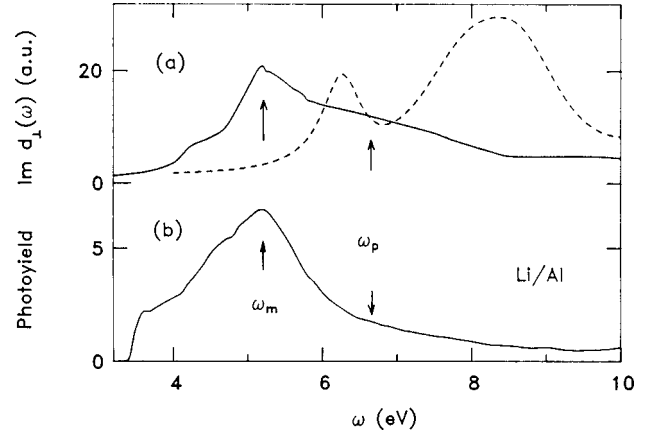


FIG. 1. (a) Calculated TDLDA excitation spectrum $\text{Im } d_{\perp}(\omega)$ for $c=2$ Li(110) on jellium substrate corresponding to Al. Solid curve, three-dimensional Li layer; dotted curve, spectrum for equivalent jellium overlayer. The frequency of the Li multipole surface plasmon is $\omega_m \approx 5.2$ eV, that of the bulk plasmon $\omega_p = 6.7$ eV. The corresponding jellium values are 6.3 and 8.4 eV, respectively. (b) Measured photoyield spectrum for Li on Al(111) for $c = 2$.

for $d_{\parallel}(\omega)$, except that we now incorporate the partial-core correction to the exchange-correlation potential²⁷ both in the ground state and response calculations.

III. RESULTS AND COMPARISON WITH EXPERIMENT

Figure 1(a) shows the calculated surface excitation spectrum $\text{Im } d_{\perp}(\omega)$ for two Li(110) layers on a jellium substrate ($r_s = 2.07$) corresponding to Al. Also shown is the analogous spectrum for the equivalent jellium overlayer of Li ($r_s = 3.25$). In this model a similar double-peak spectrum is found as for Na and K on Al:^{8,9} a bulklike overlayer plasmon near 8.4 eV and a multipole surface plasmon near 6.3 eV. The comparison with the results for the three-dimensional Li overlayer indicates that the Li potential lowers the frequencies of both modes by about 1 eV: the multipole mode now appears at $\omega_m \approx 5.2$ eV while the bulklike excitation is centered roughly at $\omega_p \approx 7$ eV. In addition, the Li potential gives rise to new single-particle transitions which predominantly broaden the overlayer volume plasmon. In Fig. 1(b) we give the measured photoyield spectrum for $c=2$ Li on Al(111) in the unreconstructed low-temperature phase.⁷

The comparison of the calculated Li spectra with experiment suggests that the lattice effects on the overlayer excitations are significant and that they are qualitatively described within the TDLDA, provided the three-dimensional nature of the electronic structure is taken into account. Evidently, the jellium model for Li overlayers is inappropriate. As illustrated in Fig. 2, a one-dimensional overlayer model that includes the corrugation normal to the surface but not within the atomic planes is also insufficient. In this case, the Li potential is replaced via a sinusoidal potential of the form $v(z) = v_0[1 - \cos(2\pi z/a)]$, where a is the spacing between Li(110) planes. The constant $v_0 = 2.8$ eV corresponds to the (110) component of the Li bulk potential.^{28,29} Since v_0 is positive, the potential reaches a maximum at the lattice planes. The surface and interface potential barriers are derived from a jellium overlayer LDA calculation. Figure 2

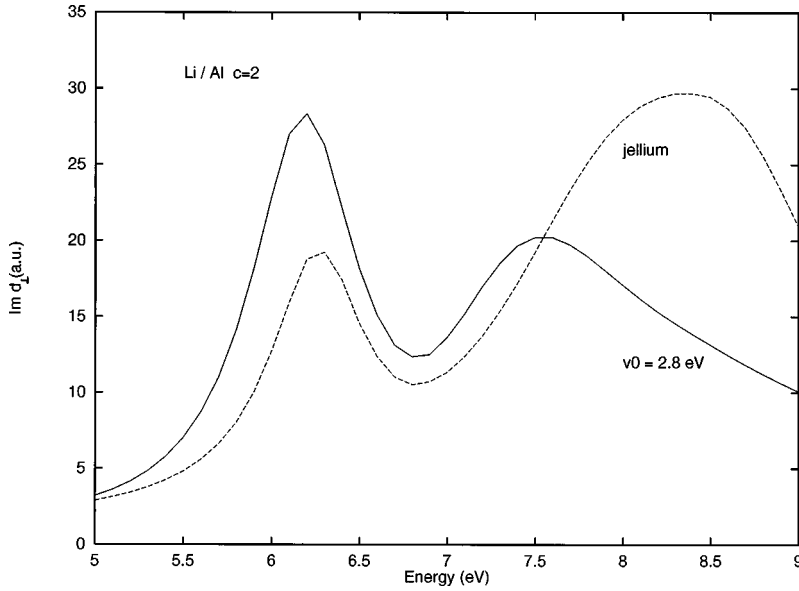


FIG. 2. Calculated TDLDA excitation spectrum $\text{Im } d_1(\omega)$ for $c=2$ Li(110) on jellium substrate corresponding to Al. Solid curve, one-dimensional Li layer ($v_0=2.8$ eV); dashed curve, spectrum for equivalent jellium overlayer ($v_0=0$).

demonstrates that this one-dimensional model for Li greatly underestimates the lattice effects. In particular, the bulklike overlayer plasmon is too sharp. The comparison with the three-dimensional results shown in Fig. 1 suggests that the single-particle transitions associated with the lateral corrugation of the Li potential contribute appreciably to the observed position and width of this mode. In fact, as the data show, for $c=2$ the frequency and width are similar to those in bulk Li [$\omega_p=6.7$ eV, $\Gamma_p=2.5$ eV (Ref. 20)].

Although the identification of the main peak observed in the Li spectra is by no means obvious, the sequence of calculated overlayer spectra reveals a clear evolution: As we proceed from the jellium model to the one-dimensional corrugated potential and finally to the realistic three-dimensional Li potential, it is rather easy to track the multipole and bulklike Li modes. Both excitations gradually shift down, but the upper bulklike plasmon is significantly more broadened than the lower multipole surface plasmon. On the basis of this pattern found in the TDLDA calculations, we are confident that our peak assignment is indeed correct.

As pointed out in the Introduction, available surface excitation spectra indicated that the multipole plasmon is a fragile surface mode easily suppressed by strong potentials. In particular, previous electron energy loss data on Li (Ref. 17) provided no evidence for this surface excitation. On the other hand, the frequency of the usual monopole surface plasmon was found to be about 25% lower than the value for the equivalent homogeneous electron gas. Also, the dispersion with q_{\parallel} is very much flatter than predicted by the jellium model. It is therefore surprising that the theoretical and experimental yield spectra shown in Fig. 1 are dominated by the Li multipole mode while the bulklike overlayer plasmon is much weaker.

To explain this behavior we show in Fig. 3 the fluctuating charge densities near $\omega_m \approx 5.2$ eV and $\omega_p \approx 6.7$ eV. Evidently, the bulklike mode corresponds to a standing wave that is fully exposed to the overlayer potential. In fact, as pointed out above, the single-particle transitions created by only two Li layers make both the frequency and width of this mode surprisingly similar to those of the Li volume plasmon. The multipole charge, on the other hand, has its main weight

near the adsorbate-vacuum interface. Only weak Friedel oscillations extend towards the adsorbate-substrate interface. Thus, this mode couples less well to the lattice than the bulklike plasmon, so that decay via interband excitations is accordingly weaker. In principle, one should be able to detect this mode also in photoyield spectra on semi-infinite Li. In the electron energy-loss data,¹⁷ the multipole plasmon should also exist, but it seems to be hidden in the tail of the intense and rather broad monopole peak.

We note here that both overlayer modes represent surface excitations of the adsorbate/substrate system. Moreover, both modes couple to electron-hole pairs generated near the adsorbate interfaces and via the lattice. This coupling differs because of the different spatial distributions of the fluctuating densities. The multipole character of the lower mode is partly obscured by the Friedel oscillations and by the externally driven nature of the response. It would be interesting to perform calculations at complex frequencies to determine the spatial characteristics of the true eigenmodes.

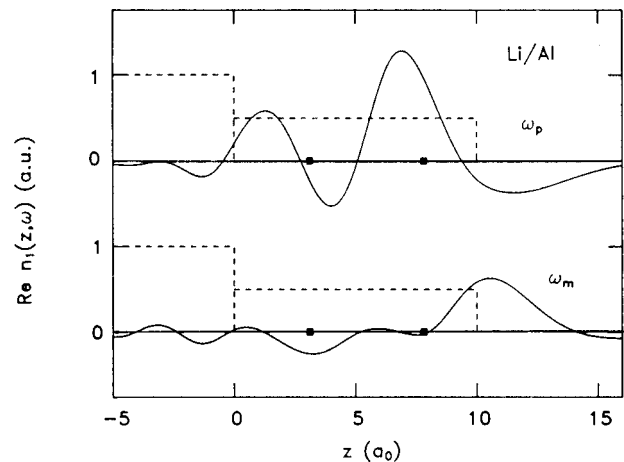


FIG. 3. Laterally averaged fluctuating charge density $n_1(z, \omega)$ (real part) for two Li(110) layers on Al. Upper curve, standing wave associated with bulklike overlayer plasmon; lower curve, multipole surface plasmon. The dots denote the positions of the Li atomic planes. The overlayer is located roughly in the region $0 \leq z \leq 10$ a.u. The substrate occupies the half-space $z \leq 0$.

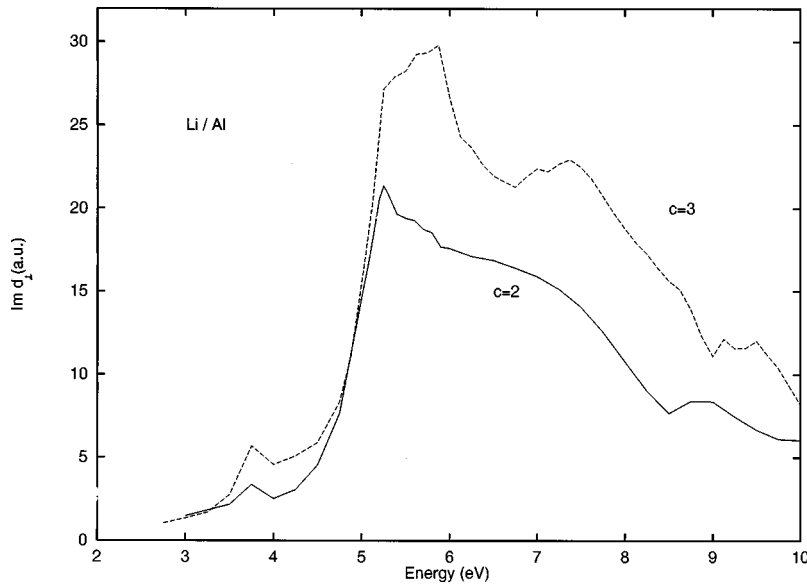


FIG. 4. Calculated TDLDA excitation spectrum $\text{Im } d_{\perp}(\omega)$ for three-dimensional Li(110) on jellium substrate corresponding to Al. Solid curve, $c=2$; dashed curve, $c=3$.

According to the experimental results given in Ref. 7, the yield spectra for Li overlayers on Al change only gradually with increasing coverage. For $c > 2$, the Li multipole mode near 5.2 eV remains the dominant spectral feature. The shoulder in the 6–8 eV range first becomes slightly stronger and beyond about 5 ML its intensity steadily diminishes. This behavior is consistent with theoretical expectations since the absorption cross section of a semi-infinite metal is approximately proportional to $(1 - \omega^2/\omega_p^2) \text{Im } d_{\perp}(\omega)$, i.e., it reaches a minimum at ω_p .¹³ In order to verify that the Li excitations discussed above for $c=2$ also hold for thicker overlayers, we have performed TDLDA calculations for three Li(110) layers on Al. The comparison with the results for $c=2$ is shown in Fig. 4. Although there are appreciable changes in detail, the overall picture remains the same: The multipole surface plasmon is the dominant feature and the bulklike Li mode is much broader and less intense. For $c=3$ the spectral peaks are slightly sharper than for $c=2$, presumably, because the modes are spatially better decoupled and therefore less broadened due to mutual interference.

Figure 5 shows the induced density for $c=3$ Li(110) on Al. As for $c=2$, the multipole mode has most of its weight concentrated close to the adsorbate-vacuum interface with Friedel oscillations extending farther inside. The bulklike plasmon, on the other hand, has pronounced standing-wave character across the entire overlayer. These results further support our picture that the multipole mode couples less to single-particle transitions generated by the lattice potential than the bulklike mode.

In the experiments, the atomic structure of the chemisorbed Li layers is not well known. To estimate the effect of different adsorption geometries on the excitation spectra, we have also carried out calculations for the Li(001) geometry (Fig. 6). The TDLDA results for this structure reveal a slightly larger damping of the Li bulklike mode than for (110). This is plausible since the interplanar spacing and distance from the jellium edge are shorter. Thus the (001) overlayer is more compact, implying stronger decay of the bulklike mode at the boundaries. On the other hand, the shape of the multipole peak is similar for both geometries because it is less affected by the lattice potential. Since the Li overlayers

in the experiment revealed no clear LEED pattern, it is likely that a mixture of (001) and (110) overlayer geometries contributes to the measured yield spectra.

In order to ascertain the sensitivity of the calculated Li spectra to the dynamical correlations included in the TDLDA treatment, we have also performed response calculations within the random-phase approximation (RPA). The ground-state electronic properties are described using the LDA, but the exchange-correlation contributions to the induced complex potential are neglected. Figure 7 shows the comparison of the spectra for $c=2$ Li(110) and Li(001) on Al with the corresponding TDLDA results. Since exchange-correlation terms tend to reduce the strength of the bare Coulomb interaction, the main effect of the RPA is a shift of spectral weight towards higher frequencies. At the same time, the fluctuating multipole charge is pushed slightly inwards, enhancing the overlap with the Li lattice potential. For the (110) geometry, these effects lead to a strong mixing of the multipole and bulklike overlayer modes, so that the peak near ω_m disappears, in conflict with the data. For the (001) geometry, the bulklike mode is weaker, so that the multipole peak remains visible. However, it is now shifted to about 5.6 eV, i.e., about 0.4 eV higher than observed experimentally. We conclude from this comparison that the dynamical correlations governing the Li overlayer excitations are better described within the TDLDA than in the RPA.

Before closing this section, we discuss the surface excitation spectrum induced by a uniform electric field parallel to the surface. Figure 8 shows the calculated $\text{Im } d_{\parallel}(\omega)$ for two Li (110) layers on a jellium substrate ($r_s = 2.07$). The xx and yy components are associated with the applied field oriented in the $[\bar{1}10]$ and $[001]$ directions, respectively. Due to the interband transitions induced by the large Li pseudopotential, the calculated $\text{Im } d_{\parallel}(\omega)$ is enhanced by one order of magnitude as compared with that for the Na overlayers on the same jellium substrate.⁹ Nevertheless, it is rather featureless in the energy range of Li excitations, and still one order of magnitude weaker than the absorption due to the many-body screening processes associated with the normal component of the electric field. Thus, we can conclude that the main

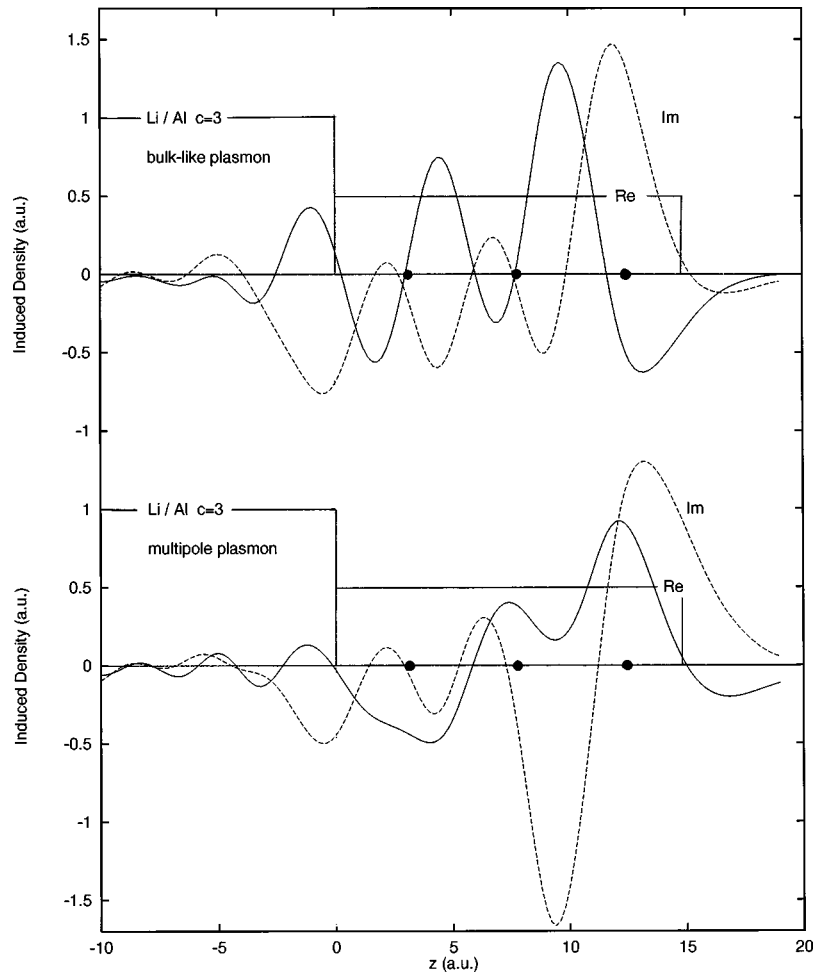


FIG. 5. Laterally averaged fluctuating charge density $n_1(z, \omega)$ for three Li(110) layers on Al. Upper curves, standing wave associated with bulklike overlayer plasmon; lower curves, multipole surface plasmon. Solid lines, real part; dashed lines, imaginary part. The dots denote the positions of the Li atomic planes. The overlayer is located roughly in the region $0 \leq z \leq 15$ a.u. The substrate occupies the half-space $z \leq 0$.

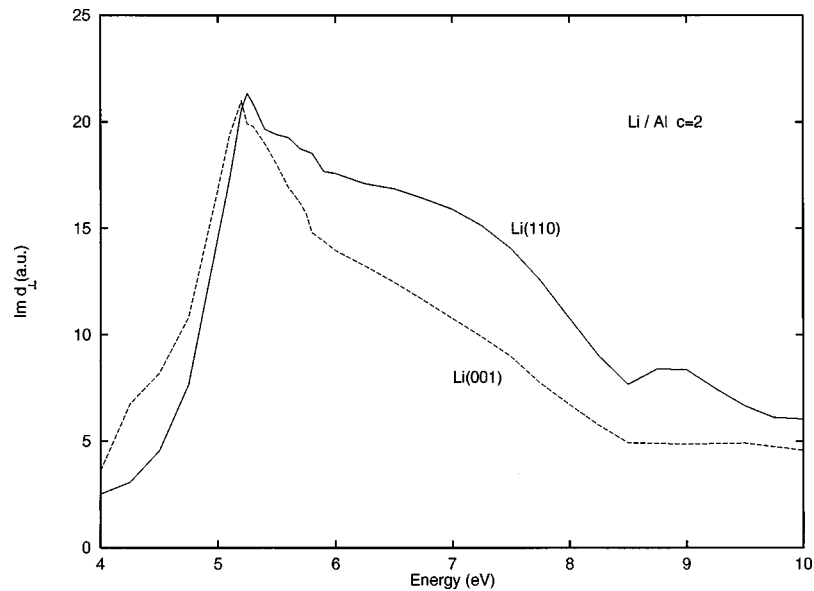


FIG. 6. Calculated TDLDA excitation spectrum $\text{Im } d_{\perp}(\omega)$ for three-dimensional Li layers on jellium substrate corresponding to Al. $c = 2$. Solid curve, Li(110); dashed curve, Li(001).

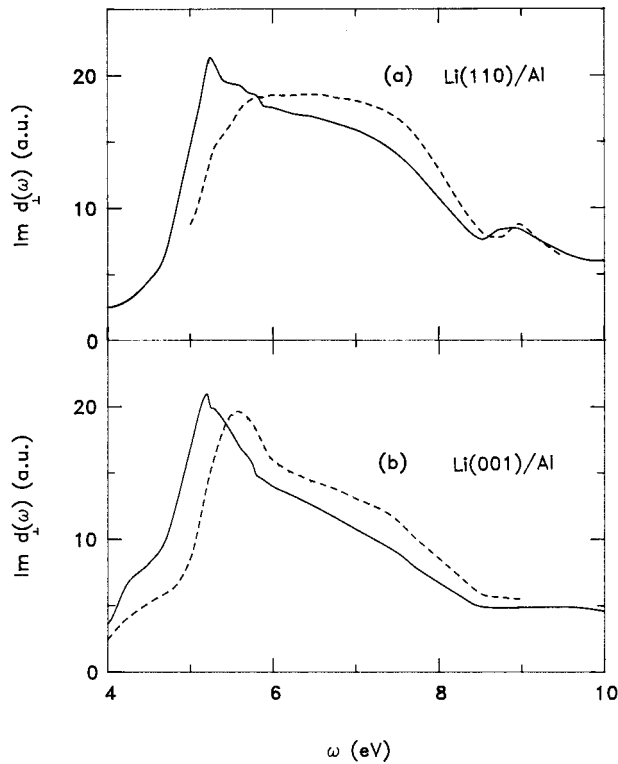


FIG. 7. Calculated TDLDA excitation spectrum $\text{Im } d_{\perp}(\omega)$ for three-dimensional Li layers on Al. $c=2$. (a) (110) geometry, (b) (001) geometry. Solid curves, TDLDA; dashed curves, RPA response.

peak observed in the recent photoyield experiment⁷ arises from the Li multipole surface plasmon.

IV. SUMMARY

We have performed a detailed analysis of the electronic excitations in Li layers adsorbed on Al. Because of the strong ionic potential of Li, the jellium model is inadequate and a fully three-dimensional dynamical response calculation must be carried out. For $c=2$, only one main Li collective excitation is found, corresponding to the Li multipole surface plasmon. The bulklike overlayer plasmon is strongly suppressed and broadened. This behavior is in striking contrast to Na and K overlayer spectra, which reveal clear double peaks near ω_m and ω_p . The TDLDA results for realistic Li adlayers agree qualitatively with measured photoyield data for Li on Al(111), which exhibit only one dominant Li-induced spectral feature. The Li bulklike mode appears only

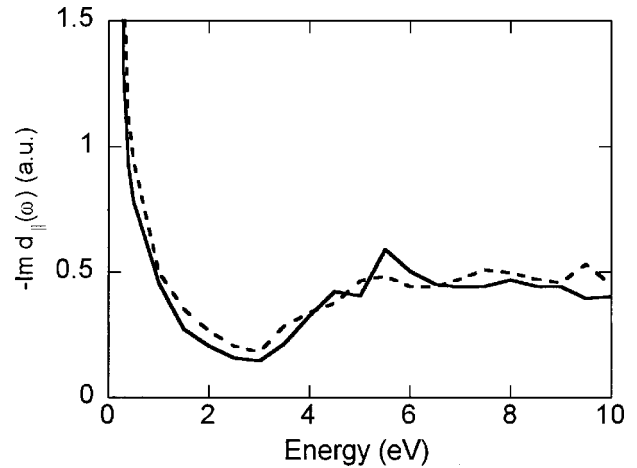


FIG. 8. Calculated TDLDA excitation spectrum $\text{Im } d_{\parallel}(\omega)$ for $c=2$ Li(110) on jellium substrate corresponding to Al. The xx (solid line) and yy (dashed line) components are associated with the applied field oriented in the $[\bar{1}10]$ and $[001]$ directions, respectively.

as a weak shoulder on the high-frequency side of the multipole peak. We conclude therefore that, despite the strong Li potential, the multipole surface plasmon is a well-defined collective excitation. In electron energy-loss spectra¹⁷ it was not possible to detect this mode since it is hidden in the tail of the monopole surface plasmon. The multipole mode should, however, be observable in photoyield spectra of single-crystal Li(110) and Li(001) surfaces.

In the present work we have focused on the excitations in Li adlayers adsorbed on Al at low temperatures. Thus, surface reconstruction and substitutional adsorption is avoided. Li/Al photoyield data taken at room temperature instead show that the Li-induced spectral weight is greatly diminished.³⁰ Similar effects are observed in yield spectra for Na and K on Al,³⁰ as well as in EELS data for K and Cs on Al (Ref. 1) and K on Al.³ The influence of substitutional adsorption on the collective modes of alkali overlayers is the topic of the second paper of this series.³¹

ACKNOWLEDGMENTS

This work was partially supported by European Community Grant No. CII *-CT93-0059 (DG 12 HSMU) and by the Japanese Society for the Promotion of Science. A.L. would like to thank the Japanese Society for the Promotion of Science for support. H.I. would like to thank the Alexander von Humboldt Stiftung for support during his stay in Jülich.

¹For a list of references, see H. Kondoh and H. Nozoye, *Surf. Sci.* **329**, 32 (1995); G. Chiarello, A. Cupolillo, A. Amoddeo, L. S. Caputi, L. Capagno, and E. Colavita, *Phys. Rev. B* **55**, 1376 (1997).

²A. Carlsson, D. Claesson, S.-Å. Lindgren, and L. Walldén, *Phys. Rev. Lett.* **77**, 346 (1996), and references herein.

³D. Heskett, E. Lundgren, R. Nyholm, and J. N. Andersen, *Phys. Rev. B* **52**, 12 366 (1995).

⁴For an overview, see T. Aruga and Y. Murata, *Prog. Surf. Sci.* **31**,

61 (1989); *Physics and Chemistry of Alkali Metal Adsorption*, edited by H. P. Bonzel, A. M. Bradshaw, and G. Ertl (Elsevier, Amsterdam, 1989).

⁵A. Liebsch, *Electronic Excitations at Metal Surfaces* (Plenum, New York, 1997).

⁶B. O. Kim, E. W. Plummer, and A. Liebsch (unpublished).

⁷S. R. Barman, K. Horn, P. Häberle, H. Ishida, and A. Liebsch, *Phys. Rev. B* **57**, 6662 (1998).

⁸A. Liebsch, *Phys. Rev. Lett.* **67**, 2858 (1991).

- ⁹H. Ishida and A. Liebsch, Phys. Rev. B **45**, 6171 (1992).
- ¹⁰A. Zangwill and P. Soven, Phys. Rev. A **21**, 1561 (1980).
- ¹¹J. Monin and S. G. A. Boutry, Phys. Rev. B **9**, 1309 (1974).
- ¹²H. E. Levinson, E. W. Plummer, and P. J. Feibelman, Phys. Rev. Lett. **43**, 952 (1979); R. A. Bartynski, E. Jensen, T. Gustafsson, and E. W. Plummer, Phys. Rev. B **32**, 1921 (1985).
- ¹³P. J. Feibelman, Prog. Surf. Sci. **12**, 287 (1982).
- ¹⁴N. D. Lang, Phys. Rev. B **4**, 4234 (1971).
- ¹⁵L. Kleinman and D. M. Bylander, Phys. Rev. Lett. **48**, 1425 (1982).
- ¹⁶K.-D. Tsuei, E. W. Plummer, A. Liebsch, K. Kempa, and P. Bakshi, Phys. Rev. Lett. **64**, 44 (1990); K.-D. Tsuei, E. W. Plummer, A. Liebsch, E. Pehlke, K. Kempa, and P. Bakshi, Surf. Sci. **247**, 302 (1991).
- ¹⁷P. D. Sprunger, G. M. Watson, and E. W. Plummer, Surf. Sci. **269/270**, 551 (1992).
- ¹⁸R. Contini and J. M. Layet, Solid State Commun. **64**, 1179 (1987); G. Lee, P. T. Sprunger, E. W. Plummer, and S. Suto, Phys. Rev. Lett. **67**, 3198 (1991); M. Rocca and U. Valbusa, *ibid.* **64**, 2398 (1990). Recent loss spectra on Ag do not show separate monopole and multipole modes but a slight variation of the shape of the main loss feature with incident energy: F. Morosco, M. Rocca, V. Zielasek, T. Hildebrandt, and M. Henzler, Phys. Rev. B **54**, R14 333 (1996).
- ¹⁹B. O. Kim, G. Lee, E. W. Plummer, P. A. Dowben, and A. Liebsch, Phys. Rev. B **52**, 6057 (1994).
- ²⁰T. A. Callcott and E. T. Arakawa, J. Opt. Soc. Am. **64**, 829 (1974).
- ²¹B. N. J. Persson and A. Apell, Phys. Rev. B **27**, 6058 (1983).
- ²²J. T. Lee and W. L. Schaich, Phys. Rev. B **44**, 13 010 (1991).
- ²³A. Liebsch, G. Benemanskaya, and M. Lapushkin, Surf. Sci. **302**, 303 (1994).
- ²⁴H. Ishida, Phys. Rev. B **52**, 10 819 (1995).
- ²⁵J. E. Inglesfield, J. Phys. C **14**, 3795 (1981). As for the application of the embedding approach to atomic overlayers on jellium, see H. Ishida, Phys. Rev. B **42**, 10 899 (1990).
- ²⁶H. Ishida, Phys. Rev. B **49**, 14 610 (1994).
- ²⁷S. G. Louie, S. Froyen, and M. L. Cohen, Phys. Rev. B **26**, 1738 (1982).
- ²⁸K. Burke and W. L. Schaich, Phys. Rev. B **48**, 14 599 (1993).
- ²⁹H. Ishida and A. Liebsch, Phys. Rev. B **54**, 14 127 (1996).
- ³⁰S. R. Barman, K. Horn, and P. Häberle (unpublished).
- ³¹H. Ishida and A. Liebsch, following paper, Phys. Rev. B **57**, 12 558 (1998).